

# Fabrication of SiNWs/PEDOT:PSS Heterojunction Solar Cells

A. A. Abdul-Hameed<sup>1</sup>, B. Ali<sup>1</sup>, H. F. Al-Taay<sup>2</sup> and M. A. Mahdi<sup>1,\*</sup>

\*mazinauny74@yahoo.com

Received: July 2019

Revised: September 2019

Accepted: December 2019

<sup>1</sup> Department of Physics, College of Science, University of Basrah, Basrah, Iraq.

<sup>2</sup> Department of Physics, College of Sciences for Women, University of Baghdad, Baghdad, Iraq.

DOI: 10.22068/ijmse.17.1.69

**Abstract:** Silicon nanowires (SiNWs) are synthesized through a metal-assisted chemical etching (MACE) method using Si (100) substrates and silver (Ag) as a catalyst. Scanning electron microscope (SEM) images confirmed that the length of prepared SiNWs was increased when etching time increased. The prepared SiNWs demonstrated considerably low light reflectance at a wavelength range of 200–1100 nm. The photoluminescence (PL) spectra of the grown SiNWs showed a broad emission band peaked at a wavelength of about 750 nm. A solar cell and photodetector based on heterojunction SiNWs/PEDOT:PSS were fabricated using SiNWs that prepared with different etching time and its J–V, sensitivity, and time response were investigated. The conversion efficiency of the fabricated solar cell was increased from 0.39% to 0.68% when wire length decreased from 24  $\mu\text{m}$  to 21  $\mu\text{m}$ , respectively. However, the sensitivity of the heterojunction SiNWs/PEDOT:PSS photodetector was decreased from 53774% to 36826% when wire length decreased from 24  $\mu\text{m}$  to 21  $\mu\text{m}$ , respectively.

**Keywords:** Silicon nanowires, PEDOT, Solar cell, Photodetector, Organic/inorganic device.

## 1. INTRODUCTION

One-dimensional nanostructured semiconductors such as nanowires are widely used to fabricate optoelectronic devices like a solar cell and photosensors due to its unique properties that depend on dimensionality, size reduction, quantum confinement, and slow electron-hole recombination [1]. Nanowires are essential to interconnection and function units used to fabricate electronic, electrochemical, optoelectronic, and electromechanical nanodevices. The development of one-dimensional nanostructures with controlled dimensional morphologies, phase purity, and chemical compositions has been slow because of the difficulties in synthesizing and manufacturing them [2]. Silicon nanowires (SiNWs) have increasingly received attention in recent years due to their diverse optoelectronic applications, such as photovoltaics, photodetection, and storage [3-5]. One of the most important properties of SiNWs is the ability to change from an indirect bandgap to a direct one through the quantum confinement effect [6]. Therefore,

SiNWs have been used to develop thin-film silicon solar cells for the enhancement of light trapping and increasing conversion efficiency [6]. Optical sensors or photodetectors are the main component of many devices that convert light to electrical signals. Photodetectors have many applications, such as flame and radiation detection like oil-burning furnaces as safety features [7], and in the security systems like near-infrared camera for night-vision [8]. However, photodetectors can be prepared in several forms such as photodiodes, photoconductive with main two configurations, metal–semiconductor–metal photodetectors, and Schottky photodiodes [9]. The preparation of SiNWs by the metal-assisted electroless etching method is adopted [10, 11]. The silver (Ag) ions in an ionic solution of hydrofluoric acid (HF) and hydrogen peroxide ( $\text{H}_2\text{O}_2$ ) have been used to prepare the arrays of SiNWs from single crystal wafers [12]. Furthermore, MACE is a simple, low cost, and powerful semiconductor etching technique that can produce high aspect ratio semiconductor nanostructures. Therefore, fabrication of photosens-

ing devices such as solar cells and photosensors based on single crystalline SiNWs are promising to obtain good efficiency and fast response. Herein, solar cells and photosensor based on SiNWs/PEDOT:PSS heterojunction are prepared and their I-V and photoelectrical characteristics are investigated.

## 2. EXPERIMENTAL

SiNWs are grown through a metal-assisted chemical etching (MACE) method using n-type single-crystalline silicon Si (100) wafers as substrates. The substrates were cleaned by ultrasonic bath with a sulfuric acid ( $H_2SO_4$ ), ethanol ( $C_2H_5OH$ ), and deionized water (DI). Then, the  $SiO_2$  layer is removed from the surface of Si (100) substrates by immersing it in 5 % of hydrofluor-

ic acid (HF) for 30 s. Silver (Ag) nanoparticles are used as catalyst for the preparation of SiNWs on the surface of the Si (100) substrates. Ag nanoparticles are synthesized on the surface of the Si (100) wafers by inserting it inside a liquid containing 0.023 mol/L of  $AgNO_3$  and HF (40%) for 90 s. To grow SiNWs, Si (100) substrates that covered by Ag nanoparticles inserted in a liquid contains equivalent molar concentrations of  $H_2O_2$  and HF with different etching time (30 min, 1 h) at room temperature. After the preparation process was done, samples were washed by DI and placed in a diluted nitric acid ( $HNO_3$ ) for 1 min to remove Ag nanoparticles from the surface of the grown SiNWs. To fabricate solar cells devices, aluminum (Al) metal was deposited onto the back of the samples by a thermal evaporation technique. The SiNWs/PEDOT:PSS

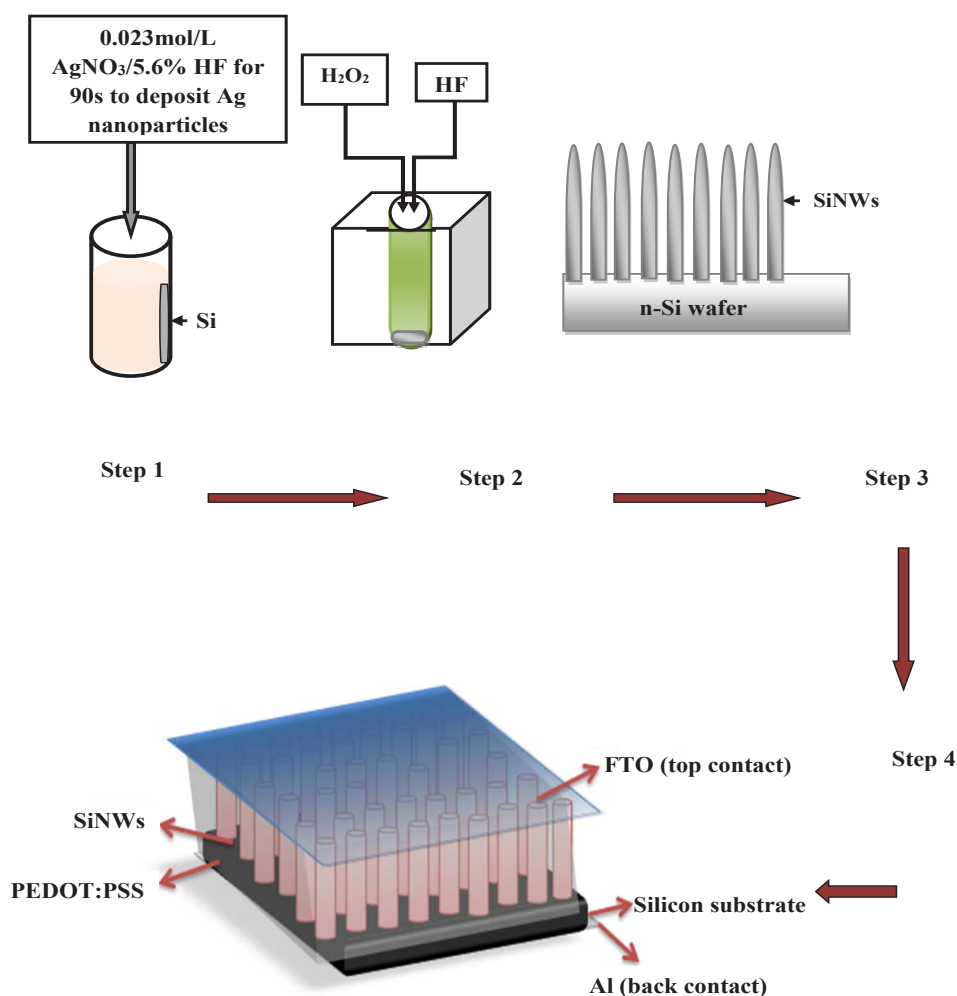


Fig.1. Preparation steps of SiNWs grown by metal assisted chemical etching method and SiNWs/PEDOT:PSS heterojunction

heterojunction was fabricated by a spin-coating (3000 rpm) of PEDOT:PSS (0.5 wt%:0.8 wt%, with 1.3 wt % dispersion in H<sub>2</sub>O, Sigma-Aldrich) on the prepared SiNWs. Fluorine-doped tin oxide (FTO)-coated glass with sheet resistance of 15 Ω/sq supplied by Kaivo-China was used as an electrode and allowing light to pass through it toward the active layer. The FTO-glass is pressed onto the SiNWs with a mechanical force so that the polymer sticks to the nanowire. The solvent from the polymer is removed through heat treatment, which also results in a good junction between the SiNWs and polymer and considerably decreases series resistance. The junction of the prepared SiNWs/PEDOT:PSS heterojunction is enhanced by heating it at 100 °C for 1 h. Figure 1 shows the preparation procedure of SiNWs grown through the MACE method. The surface morphology of the prepared SiNWs is studied with a field emission scanning electron microscopy (FESEM) equipment (Zeiss Supra 55VP, Germany). The optical properties of the prepared

SiNWs are investigated using a photoluminescence (PL) spectrum, which is tested through Perkin-Elmer LS-3 fluorescence spectroscopy and reflectivity spectra obtained with a spectrophotometer (Shimadzu UV-1800). The current density–voltage (J–V) characteristics are measured with a Keithley 2400 electrometer under dark and illumination conditions.

### 3. RESULTS AND DISCUSSION

#### 3.1 Morphology

Fig. 2 shows the FESEM images of the top-view and cross-sectional of the grown SiNWs prepared at a different time of etching. The diameters of the grown SiNWs prepared with equivalent concentrations of HF:H<sub>2</sub>O<sub>2</sub> for 30 min and 1 h of etching time ranged from 40 nm to 350 nm, but the wire length increased from 21 μm to 24 μm when increasing the etching time from 30 min to 1 h. However, wire diameter and length gen-

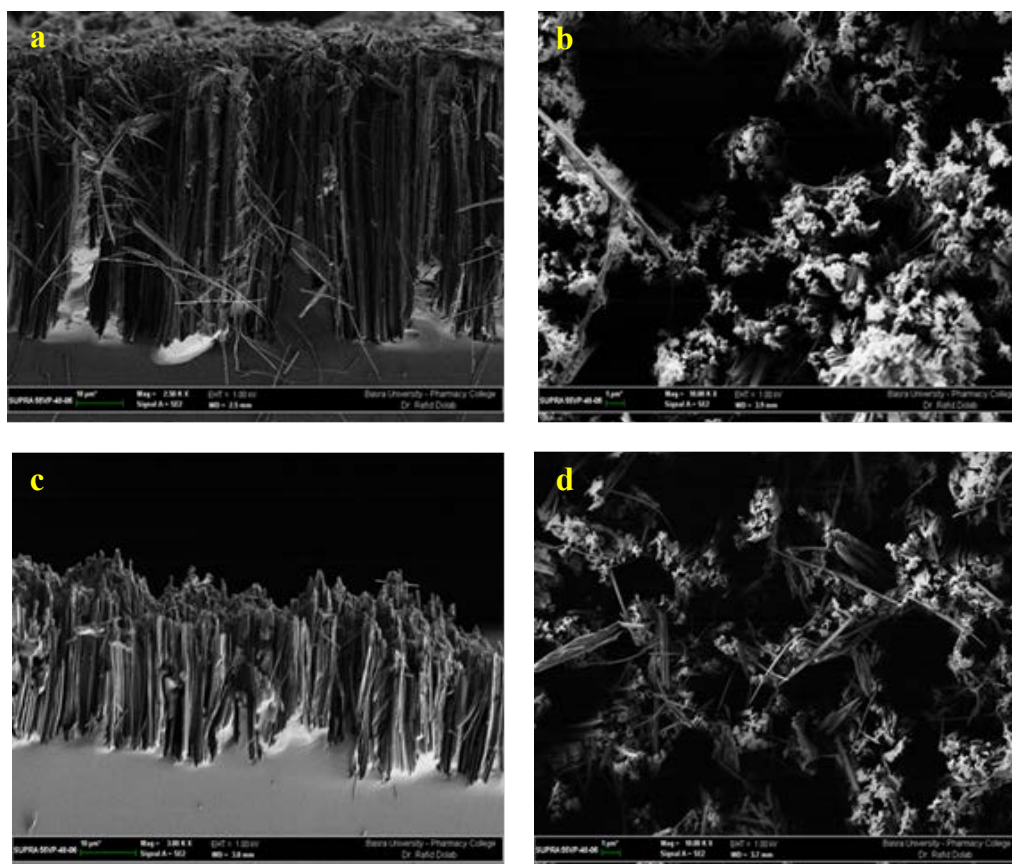


Fig. 2. FESEM images of SiNWs grown using etching time of (a and b) for 1h, (c and d) for 30 min

**Table 1.** Preparation parameters of SiNWs grown by metal assisted chemical etching method.

Sample	$\lambda$ (nm) emission	Time	Diameter (nm)	Length ( $\mu$ m)
S1	750	1h	40-350	24
S2	749	30min		21

erally were increased with etching time. Tips of prepared SiNWs were conglomerated and seem as sheaves. The reasons for the conglomeration of SiNWs synthesized by MACE are: (1) the SiNWs collapse because they are too long, and (2) the strong forces, such as dangling bonds and electrostatic charge on the freshly formed surfaces, induce mutual attraction [13]. However, the electroless deposition method can only prepare randomly distributed SiNWs with a varied diameter [14]. Srivastava et al. were the first to prepare SiNWs through the MACE method using Ag nanoparticles as a catalyst and they found that the length and diameter of the grown SiNW depend on the etching time where the length increased from 1  $\mu$ m to 12  $\mu$ m and the diameter enlarged from 50 nm to 300 nm when the etching time was increased from 5 to 45 min [15]. Qi et al. grew a vertically aligned SiNW array using Ag as a catalyst. They noted that the lengths of the SiNWs prepared at 15, 30, 45, and 60 min increased from 20  $\mu$ m to 40  $\mu$ m [16].

### 3.2. Optical Properties

#### 3.2.1. Photoluminescence (PL) Spectra

Fig. 3 explains the PL spectra of the SiNWs grown using equivalent concentrations of HF:H<sub>2</sub>O<sub>2</sub> and different etching times. In SiNWs prepared for 30 min and 1 h, the PL bands appeared at 749 and 750 nm, respectively. The PL emission bands of the grown SiNWs blue-shifted relative to the optical bandgap of bulk crystalline silicon (c-Si). The optical bandgaps of nanostructures expand when particle size is decreased because of the quantum confinement effect [17]. Optical bandgap can be obtained with the following equation [18]:

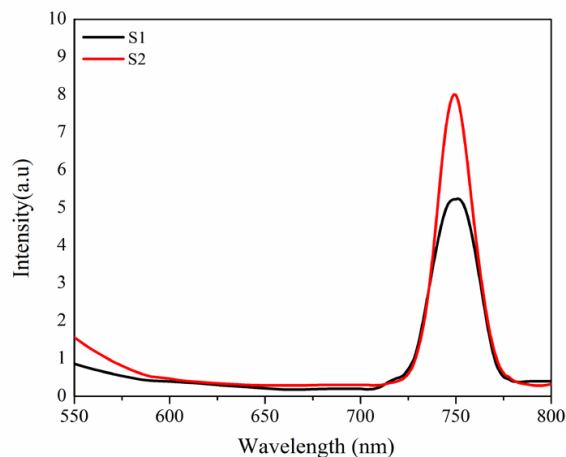


**Fig. 3.** PL spectra of SiNWs grown using HF:H<sub>2</sub>O<sub>2</sub> concentration and etching time of (S1) 1hr, (S2) 30min.

where  $E$  ( $\sim 1.66$  eV) is the optical bandgap obtained from the PL spectrum,  $E_0$  is the c-Si bandgap (1.12 eV), and  $d$  is the diameter of SiNWs. The calculated diameter of the prepared SiNWs was approximately 4.7 nm. However, the diameters of the grown SiNWs were larger than those calculated by Eq. 1 and the Bohr radius of excitons for crystalline Si is 5 nm. Therefore, the emission in the red wavelengths cannot be attributed to the quantum size effect and a thin layer of SiO<sub>2</sub> covering the SiNW surfaces [19]. Visible PL emission from SiNWs could be due to quantum confinement effect, interface defects between SiO<sub>2</sub> and Si, or states of Si-Oxide defect in the surface of silicon nanowires [20, 21].

$$E = E_0 + \frac{3.73}{d^{1.39}} \quad \dots 1$$

Gonchar et al. [22] prepared SiNWs through the MACE method and found that the samples emitted visible light with maximum PL intensity at 740 nm. Zhang et al. [23] synthesized SiNWs

by the MACE technique using Ag as a catalyst, and got a broad emission band at approximately 750 nm and the other two emission bands at 752 and 688 nm, respectively. Furthermore, they concluded that the bands were emitted from the silicon nanowire coated by a thin oxide layer.

### 3.2.2. Optical Reflectivity of SiNWs

Fig. 4A shows the reflectance (R) spectra of SiNWs prepared through the MACE method at different etching times. The grown SiNWs demonstrated extremely low reflectivity in the wavelength range of 200–400 nm and increased to a maximum value at a wavelength of approximately 850 nm. Compared to bulk silicon wafer, whose reflectivity spectrum reached 40% at the wavelengths longer than 400 nm, the prepared SiNWs showed a considerably low R (approximately 0.2%–0.5%) in the visible region. Very low reflectance of SiNWs can be explained by the strong light scattering and absorption, which results in partial localization (trapping) of the excited light in SiNWs array [24]. Thus, by using SiNWs to fabricate photosensor devices such as solar cell, no antireflection layer is needed. Kumar et al. prepared silicon nanowires through the MACE method and found that reflectivity value decreased to 2% in the wavelength region of 300–600 nm but increased to approximately 5% at longer wavelengths [25].

### 3.3. Photoelectrical Properties of the SiNWs/PEDOT:PSS Solar Cell

Fig. 5 displays the J–V characteristics of the heterojunction SiNWs/PEDOT:PSS solar cell prepared using different etching times under white light illumination of 50 mW/cm<sup>2</sup>. The solar cell that fabricated based on SiNWs prepared for 30 min exhibited the highest  $V_{oc}$  and  $J_{sc}$  of 0.394 V and 3.072 mA/cm<sup>2</sup>, respectively. However, a solar cell that fabricated with SiNWs length of 24  $\mu$ m unveiled  $V_{oc}$  and  $J_{sc}$  of 0.360 V and 2.087 mA/cm<sup>2</sup>, respectively. The conversion efficiency ( $\eta$ ) was measured four times for every sample and found that the highest value was 0.68% (average value was 0.59%) for the solar cell that fabricated based on 21  $\mu$ m-long SiNW. Howev-

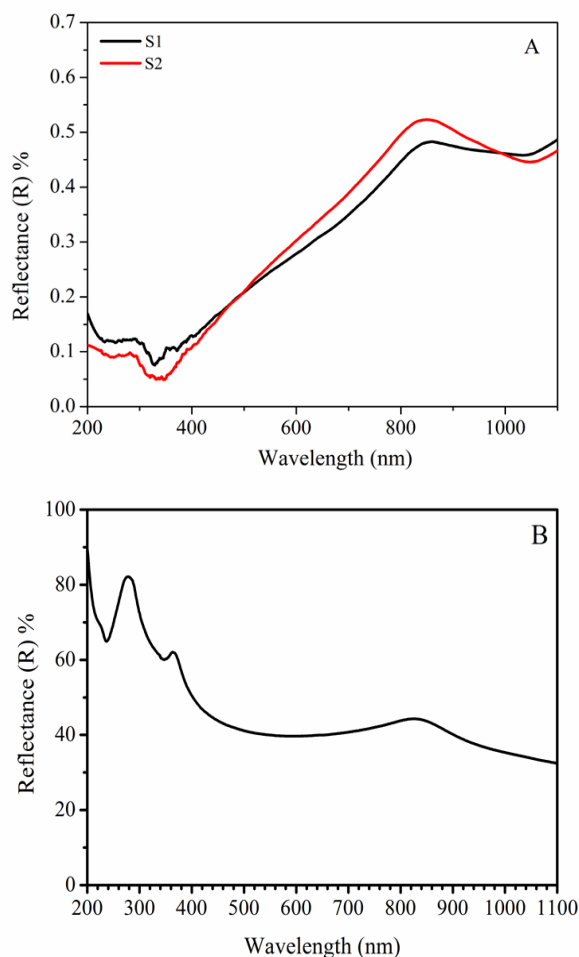


Fig. 4. Reflectance spectra of (A) SiNWs grown using an etching time of (S1) 1hr, (S2) 30min and (B) silicon wafer.

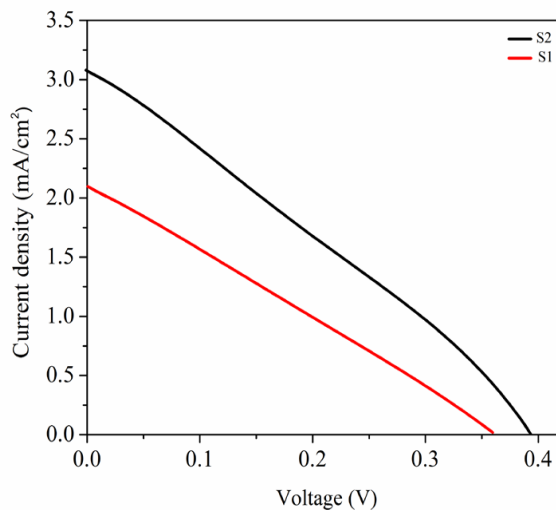


Fig. 5. J–V characteristics of heterojunction SiNWs solar cell under light with power of 50mW/cm<sup>2</sup> white light prepared using etching time of (S1) 1 h, (S2) 30 min.

er, the  $\eta$  decreased to 0.38% (average value was 0.30%) when the length of the SiNW increased to 24  $\mu\text{m}$ . The fill factor (FF) decreased from 28% to 26% when the wire length was increased from 21  $\mu\text{m}$  to 24  $\mu\text{m}$ . Series resistance ( $R_s$ ) and shunt resistance ( $R_{sh}$ ) are important parameters that can affect the solar cell output where high  $R_s$  value decreases the output voltage of a solar cell under load and therefore decreases FF.  $R_s$  should be low because high  $R_s$  value can lead to voltage increase inside the solar cell. The  $R_s$  and  $R_{sh}$  values of the samples prepared for 30 min (wire length of 21  $\mu\text{m}$ ) were 136  $\Omega$  and 344  $\Omega$ , respectively. The  $R_s$  increased to 299  $\Omega$ , and  $R_{sh}$  to 311  $\Omega$  when SiNW length was increased to 24  $\mu\text{m}$ . These changes decrease the FF from 26% to 24% and increased the conversion efficiency from 0.39% to 0.68%. However, increasing  $R_s$  value at higher etching time could be due to the increasing thickness of the  $\text{SiO}_2$  thin layer that covering SiNWs. Huang et al. prepared a hybrid

solar cell heterojunction using single crystalline silicon nanowire and P3HT:PCBM and they observed when the  $R_s$  was reduced from 18.09  $\Omega$  to 10.59  $\Omega$  the  $J_{sc}$  increased from 7.17  $\text{mA}/\text{cm}^2$  to 11.61  $\text{mA}/\text{cm}^2$  and  $\eta$  increased from 1.21% to 1.9% [26]. Woo et al. fabricated heterojunction solar cells based on ITO/PEDOT/n-SiNWs, and they found the increase in  $J_{sc}$  from 0.75  $\text{mA}/\text{cm}^2$  to 1.55  $\text{mA}/\text{cm}^2$  and FF from 32.8% to 40.6% when low resistance Si wafer was used that led to the enhancement of conversion efficiency that increased from 0.05% to 0.15% [27]. Table 2 presents the obtained output parameters of the fabricated SiNWs/PEDOT:PSS heterojunction solar cell.

### 3.4. Photoelectrical Properties of the Heterojunction SiNWs/PEDOT:PSS

Fig. 6 shows the photocurrent response of the SiNWs/PEDTO:PSS device prepared at dif-

**Table 2.** Output of prepared the heterojunction SiNWs/PEDOT:PSS solar cells.

Sample	$J_{sc}$ ( $\text{mA}/\text{cm}^2$ )	$V_{oc}$ (V)	FF%	$\eta$ %	$R_s$ ( $\Omega$ )	$R_{sh}$
S1	2.087	0.360	26	0.39	299	311
S2	3.072	0.394	28	0.68	136	344

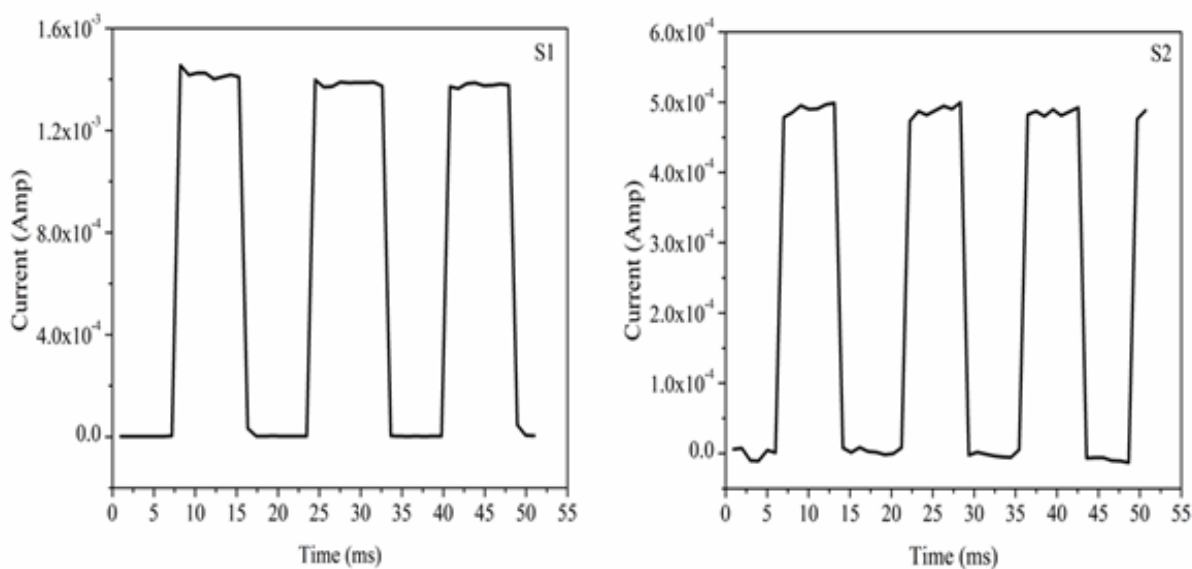


**Fig 6.** Photocurrent response of SiNWs photosensor under chopped white light with power of 50mW/cm<sup>2</sup> prepared using etching time of (S1) 1 h, (S2) ) 30 min

**Table 3.** Rise, decay times and sensitivity of SiNWs/PEDOT:PSS photosensor.

Sample	Rise time (ms)	Decay time (ms)	Sensitivity %
S1	0.8	0.9	54264
S2	0.85	0.89	36826

ferent times of etching. The photocurrent was increased to a maximum value as the light was switched ON (illumination case) and decreased to the minimum value as the light was switched OFF (dark case). The photodetector based on SiNWs that grew for 1 h exhibited the highest photocurrent of 1.46 mA whereas the photodetector that fabricated using SiNWs which grown for 30 min showed a photocurrent value of 0.498 mA.

The photosensitivity (S) of the prepared photodetectors was determined using the following equation [28]:

$$S = \frac{I_{light} - I_{dark}}{I_{dark}} \times 100\% \quad 2$$

where  $I_{dark}$  is dark current, and  $I_{light}$  represented the photocurrent. The photodetector that fabricated using SiNWs grown for 1 h showed the highest photosensitivity of 53774% while it was 36826% for the sample prepared for 30 min. However, the length of SiNWs prepared for 1 h was longer than those prepared for 30 min thus; the surface area of long wires could be improved the photosensitivity. The speed sensing of the photodetector represents an important parameter, which determines the feature of the device. Rise time ( $R_t$ ) refers to the time at which the photocurrent increases from 10% to 90% of the maximum value, whereas decay time ( $D_t$ ) represents the time for the photocurrent to decrease from 90% to 10% of the maximum value of current. The photodetector etched for 1 h was faster with  $R_t$  and  $D_t$  of 0.8 and 0.85 ms, respectively; whereas the  $R_t$  and  $D_t$  of the photodetector that etched for 30 min were 0.85 and 0.89 ms, respectively. Table 3 describes the parameters of the rise and decay times and device sensitivity.

#### 4. CONCLUSIONS

SiNWs were grown through the MACE method using Ag as a catalyst at different etching times. FESEM images showed that the length of SiNWs was increased when etching time was increased. Furthermore, synthesized SiNWs demonstrated a reflectivity of approximately 0.5% at the wavelength range of 200–1100 nm. This reflectivity value was considerably lower than that of the crystalline silicon wafer. The PL spectra showed that all prepared SiNWs emitted bands at 750 nm. The J–V characteristics of the heterojunction solar cell fabricated on the basis of SiNWs prepared using different etching time showed an increase in conversion efficiency with the decrease in wire length. The SiNWs/PEDOT:PSS photodetectors based on SiNWs prepared for 1 h showed high photosensitivity of 53774%. Furthermore, the speed sensing of all prepared photodetectors showed the fast rise and decay times of approximately 0.8 and 0.9 ms, respectively.

#### REFERENCES

1. Mahdi, M. A, Hassan, J. J, Kasim, S. J., Ng S., Hassan, Z., "Solvothermal growth of single-crystal CdS nanowires". *B Mater. Sci.*, 2014, 37, 337–345.
2. Tharmavaram, M., Rawtani, D., Pandey, G., "Fabrication routes for one-dimensional nanostructures via block copolymers". *Nano Converg.*, 2017, 4, 12-24.
3. Jia, G., Steglich, M., Sill, I., Falk F., "Core-shell heterojunction solar cells on silicon nanowire arrays". *Sol. Energy Mater. Sol. Cells.*, 2012, 96, 226-230.
4. Al-Taay, H., Mahdi, M., Parlevliet, D., Jennings, P., "Controlling the diameter of silicon nanowires grown using a tin catalyst". *Mat. Sci. Semicon. Proc.*, 2013, 16, 15-22.
5. Al-Taay, H., Mahdi, M., Parlevliet, D., Jennings, P., "Fabrication and characterization of solar cells based on silicon nanowire homojunctions". *Silicon*, 2017, 9, 17-23.

6. Al-Taay, H. F., Mahdi, M. A., Parlevliet, D., Hassan, Z., Jennings, P., "Preparation and characterization of silicon nanowires catalyzed by aluminum". *Physica E*, 2013, 48, 21-28.
7. Gottuk, D. T., Dinaburg, J. B., "Video image detection and optical flame detection for industrial applications". *Fire Technol.*, 2013, 49, 213-251.
8. Vivien, L. and Pavesi, L., "Handbook of silicon photonics". CRC Press, Taylor & Francis Group, USA, 2016, 492.
9. Omnes, F., "Introduction to semiconductor photodetectors". In *Optoelectronic Sensors*. ISTE, Arlington, VA, 2010, 1-14.
10. Hochbaum, A. I., Gargas, D., Hwang, Y. J., Yang, P., "Single crystalline mesoporous silicon nanowires". *Nano Lett.*, 2009, 9, 3550-3554.
11. Kumar, D., Srivastava, S. K., Singh, P. K., Sood, K. N., Singh, V. N., Dilawar, N., Husain, M., "Room temperature growth of wafer-scale silicon nanowire arrays and their Raman characteristics". *J. Nanoparticle Res.*, 2010, 12, 2267-2276.
12. Qiu, T, Wu, X. L., Mei, Y. F., Wan, G. L., Chu, P. K., Siu, G. G., "From Si nanotubes to nanowires: synthesis, characterization, and self-assembly". *J. Cryst. Growth*, 2005, 277, 143-148.
13. Zhang, M. L., Peng, K. Q., Fan, X, Jie, J. S., Zhang, R. Q., Lee, S. T., Wong, N. B., "Preparation of Large-Area Uniform Silicon Nanowires Arrays through Metal-Assisted Chemical Etching". *J. Phys. Chem. C*. 2008, 112, 4444-4450.
14. Vinzons, L. U., Shu, L., Yip, S., Wong, C. Y., Chan, L. H., Ho, J. C., "Unraveling the Morphological Evolution and Etching Kinetics of Porous Silicon Nanowires During Metal-Assisted Chemical Etching". *Nanoscale Res. Lett.*, 2017, 12, 385-397.
15. Srivastava, S. K., Kumar, D., Singh, P., Kar, M., Kumar, V. and Husain, M., "Excellent antireflection properties of vertical silicon nanowire arrays". *Sol. Energy Mater. Sol. Cells.*, 2010, 94, 1506-1511.
16. Qi, Y, Wang, Z, Zhang, M, Yang, F, Wang, X., "A processing window for fabricating heavily doped silicon nanowires by metal-assisted chemical etching", *J. Phys. Chem. C.*, 2013, 117, 25090-25096.
17. Mahdi, M. A., Hassan, Z., Ng, S., Hassan, J., Bakhori, S. M., "Structural and optical properties of nanocrystalline CdS thin films prepared using microwave-assisted chemical bath deposition". *Thin Solid Films*, 2012, 520, 3477-3484.
18. Lajvardi, M., Eshghi, H., Ghazi, M., Izadifard, M. and Goodarzi, A., "Structural and optical properties of silicon nanowires synthesized by Ag-assisted chemical etching". *Mat. Sci. Semicon. Proc.*, 2015, 40, 556-563.
19. Abdul-Hameed, A. A., Mahdi, M. A., Ali, B., Selman, A. M., Al-Taay, H., Jennings, P., "Fabrication of a high sensitivity and fast response self-powered photosensor based on a core-shell silicon nanowire homojunction". *Superlattices Microst.*, 2018, 116, 27-35.
20. Najar, A., Slimane, A., Hedhili, M. N., Anjum, D., Sougrat, R. and Ng, T., "Effect of hydrofluoric acid concentration on the evolution of photoluminescence characteristics in porous silicon nanowires prepared by Ag-assisted electroless etching method". *J. Appl. Phys.*, 2012, 112, 033502-033509.
21. Sivakov, V. A., Voigt, F., Berger, A., Bauer, G., Christiansen, S. H., "Roughness of silicon nanowire sidewalls and room temperature photoluminescence", *Phys. Rev. B*, 2010, 82, 125446-125451.
22. Gonchar, K., Osminkina, L., Galkin, R., Gongalsky, M., Marshov, V., Timoshenko, V. Y., Kulmas, M., Solovyev, V., Kudryavtsev, A., Sivakov, V., "Growth, structure and optical properties of silicon nanowires formed by metal-assisted chemical etching". *J. Nanoelectron. Optoelectron.*, 2012, 7, 602-606.
23. Zhang, C., Li, C., Liu, Z., Zheng, J., Xue, C., Zuo, Y., Cheng, B., Wang, Q., "Enhanced photoluminescence from porous silicon nanowire arrays". *Nanoscale Res. Lett.*, 2013, 8, 277-280.
24. Gonchar, K. A., Zubairova, A. A., Schleusener, A., Osminkina, L. A., Sivakov, V., "Optical Properties of Silicon Nanowires Fabricated by Environment-Friendly Chemistry". *Nanoscale Res. Lett.*, 2016, 11, 357-361.
25. Kumar, D., Srivastava, S. K., Singh, P., Husain, M., Kumar, V., "Fabrication of silicon nanowire arrays based solar cell with improved performance". *Sol. Energy Mater. Sol. Cells.*, 2011, 95, 215-218.
26. Huang, J. S., Hsiao, C. Y., Syu, S. J., Chao, J. J., Lin, C. F., "Well-aligned single-crystalline silicon nanowire hybrid solar cells on glass". *Sol. Energy Mater. Sol. Cells.*, 2009, 93, 621-624.
27. Woo, S., Jeong, J. H., Lyu, H. K., Jeong, S., Sim, J. H., Kim, W. H., "Hybrid solar cells with conducting polymers and vertically aligned silicon nanowire arrays: The effect of silicon conductivity", *Physica B*, 2012, 407, 3059-3062.
28. Mahdi, A. M., Hassan, J. J., Ahmed, N. M., Ng, S., Hassan, Z., "Growth and characterization of CdS single-crystalline micro-rod photodetector", *Superlattices Microst.*, 2013, 54, 137-145.